Sensors and Actuators B 230 (2016) 658–666

Contents lists available at ScienceDirect

Sensors and Actuators B: Chemical

journal homepage: www.elsevier.com/locate/snb

Development of a hydrogen sulfide end-of-service-life indicator for respirator cartridges using cobinamide

Lee A. Greenawald [a,*], Gerry R. Boss [b], Aaron Reeder [c], Suzanne Bell [d]

[a] Centers for Disease Control and Prevention/National Institute for Occupational Safety and Health/National Personal Protective Technology Laboratory/Evaluation and Testing Branch (CDC/NIOSH/NPPTL/ETB), 1095 Willowdale Road, Morgantown, WV 26505, USA
[b] Department of Medicine, 9500 Gilman Drive, University of California, La Jolla, San Diego, CA 92093 USA
[c] Centers for Disease Control and Prevention/National Institute for Occupational Safety and Health/National Personal Protective Technology Laboratory/Evaluation and Testing Branch (CDC/NIOSH/NPPTL/ETB), 626 Cochrans Mill Road, Pittsburgh, PA 15236, USA
[d] C. Eugene Bennett Department of Chemistry, 217 Clark Hall, West Virginia University, Morgantown, WV 26506, USA

ARTICLE INFO

Article history:
Received 11 November 2015
Received in revised form 2 February 2016
Accepted 26 February 2016
Available online 3 March 2016

Keywords:
Optical sensor
Diffuse reflectance
Aquohydroxocobinamide
Hydrogen sulfide
End-of-service-life indicator

ABSTRACT

An inexpensive paper-based sensor was developed for detecting low ppm concentrations of hydrogen sulfide gas. A piece of filter paper containing aquohydroxocobinamide [OH(H_2O)Cbi] was placed on the end of a bifurcated optical fiber, and the reflectance spectrum of the OH(H_2O)Cbi was monitored during exposure to 10.0 ppm hydrogen sulfide gas (NIOSH recommended exposure limit). Reaction of sulfide (HS^-) yielded an increase in reflectance from 400–450 nm, and decrease from 470–550 nm. Spectral changes were monitored as a function of time at 25, 50, and 85% relative humidity. Spectral shifts at high-er humidity suggested reduction of the Cbi(III) compound. The sensor was used to detect hydrogen sulfide breakthrough from respirator carbon beds and results correlated well with a standard electrochemical detector. The simple paper-based sensor could provide a real-time end-of-service-life alert for hydrogen sulfide gas.

1. Introduction

Persons who may be exposed to hydrogen sulfide (H_2S) in the workplace are recommended to wear a self-contained breathing apparatus (SCBA) or an air-purifying respirator (APR) fitted with NIOSH-approved cartridges for H_2S [1]. When the carbon in APR cartridges becomes saturated, the cartridge's "end-of-service-life" (ESL) has been reached. Metal oxides, among other chemical impregnants, are added to the carbon for enhanced removal of low molecular weight gases, but saturation still occurs. The carbon within a cartridge becomes saturated from the front to the back of the cartridge, ultimately leading to breakthrough—i.e., penetration of the gas through the cartridge [2]. Currently, no definitive method exists to determine when ESL occurs while a respirator is being worn. Prior to 1976, the smell or irritation of a gas was used to indicate breakthrough, but by the time a user can smell a gas, dangerous concentrations may already be present within the respirator. According to OSHA regulation 1910.134, sensory warning properties cannot be used to determine cartridge change-out [3]. Software models provided by respirator manufacturers are currently used to help users estimate when breakthrough will occur [4]. Unfortunately, the user may not be aware of unpredictable input data for the model such as types and concentrations of toxic chemicals, relative humidity, and breathing rate. In addition, most of the software models were developed from organic vapor data.

In 1984, NIOSH published standards for certifying sensors that indicate imminent breakthrough to encourage sensor development [5]. These standards provide criteria for certifying both passive and active end-of-service-life indicators (ESLIs and AESLIs, respectively [6]) and require that a sensor indicates when 90% of the carbon is saturated, without hindering normal use of the respirator [2,7]. The sensors are designed to be embedded in the back part of the carbon bed of a cartridge, enclosed in a clean environment. AESLIs are intended to provide a real-time alert (e.g., flashing LED) when the cartridge is near its maximum absorption capacity and vapor breakthrough is imminent. Current challenges in developing APR sensors are the effects of humidity, selectivity, size, weight, and power restrictions. Additionally, manufacturers prefer to limit sensor costs to about $1 per cartridge, and $20–$50 for sensor-related fixtures and electronics [5]. Only a few colorimetric and qualitative ESLIs are commercially available, e.g., for mercury vapor; these rely on subjective visual identification of a color change [8,9]. For passive colorimetric ESLIs to be effective, the user must routinely

* Corresponding author at: National Institute for Occupational Safety and Health, 1095 Willowdale Road, M/S 1904, Morgantown, WV 26505, USA.
E-mail addresses: lgreenaw@mix.wvu.edu, ilv1@cdc.gov (L.A. Greenawald).

http://dx.doi.org/10.1016/j.snb.2016.02.129
0925-4005/

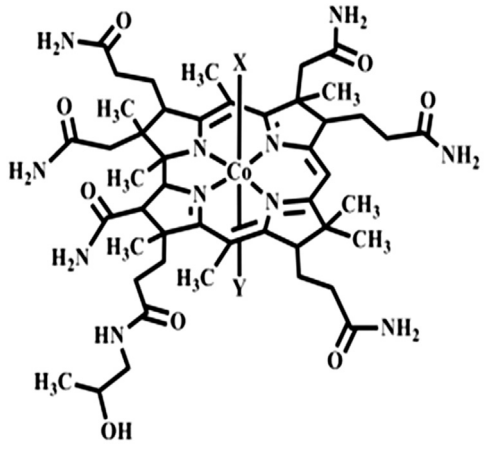

Fig. 1. Structure of cobinamide (Cbi).

monitor the sensor for color change [2]. This is inappropriate in poorly-lit environments, fogging respirators, or for color blind persons. Currently, no NIOSH-certified AESLIs exist.

H_2S is a corrosive and flammable gas that can be lethal at concentrations >500 ppm [10]. It is commonly used or produced in oil and gas refining, waste water treatment, mining, tanning and pulp and paper processing industries [11]. Both acute and chronic H_2S exposure can be injurious to humans. Known for its characteristic "rotten egg" smell, many workers believe the distinct odor is a suitable means for detecting H_2S. However, a person can become "desensitized" due to olfactory fatigue within 15 min of exposure to low H_2S concentrations (100–150 ppm) or more rapidly at higher H_2S concentrations [12]. Although early odor detection of H_2S is beneficial, NIOSH and OSHA stress that odor is not a reliable indicator, especially at elevated H_2S concentrations. Thus, appropriate respiratory protection with an ESLI is required. Although the number of fatalities associated with H_2S is not known, the recent surge in oil and gas extraction in the United States increases the occupational risk of H_2S exposure. The NIOSH C ("C" = ceiling, 10 min maximum) Recommended Exposure Limit (REL) for H_2S is 10 ppm, with an immediately dangerous to life or health concentration of 100 ppm [1]. Thus, a person should not be exposed to concentrations above 10 ppm H_2S for more than 10 min during a 10-h workday. Exposure to low H_2S concentrations can cause stress and anxiety, while high H_2S concentrations can cause loss of consciousness, permanent brain damage, or death [13].

Portable electrochemical detectors are commonly used to detect H_2S. Typical detectors have a range of 0.0–500. ppm H_2S, with limits of detection ~0.5 ppm and common resolutions of 1 ppm [14,15]. Although widely used and offering moderate to high sensitivity, electrochemical detectors and other common H_2S detection systems (e.g., gas chromatography with various detectors) are too large and costly to be useful as an ESLI incorporated into the carbon bed of a respirator. Spectroscopic detection methods offer moderate to high sensitivity, miniaturized designs, low power requirements, and detection limits in ppb–ppm range. Paper is a good substrate for real-time, low-cost sensors; it offers a bright, high-contrast backing for spectrometric applications and is highly porous with a large surface area, advantageous for rapid diffusion of gas-phase analytes. A potential disadvantage of paper is inhomogeneous coating of the indicator, which can cause diffusion and poor reproducibility.

Cobinamide (Cbi), a cobalt-centered Vitamin B_{12} derivative, is known to have a high affinity for cyanide (CN^-), but can also bind up to two sulfide (HS^-) ions [16–18] (Cbi structure is shown in Fig. 1, where the *X* and *Y* ligands can be OH^-, H_2O, HS^-, or CN^-). At neutral pH in water, Cbi exists as the mixed aquo-hydroxo complex $OH(H_2O)Cbi$, termed aquohydroxocobinamide [18]. H_2S, a reducing agent, reacts with $(H_2O)_2Cbi(III)$ in three consecutive and rapid steps[16]:

1.1. Complex formation:

$$\frac{(H_2O)_2Cbi + HS^- \rightleftarrows (HS)(OH)Cbi(III)}{(HS)(H_2O)Cbi(III)(pK_a > 10.5)}$$

1b. Addition of second HS^- at higher concentrations:

$$\frac{(HS)(OH)Cbi(III)}{(HS)(H_2O)Cbi(III) \rightleftarrows (HS)_2Cbi(III)}$$

1.2. Inner-sphere electron transfer and reduction of Cbi

$$(HS)(OH)Cbi(III)/(HS)(H_2O)Cbi(III) \rightleftarrows (H\dot{S})Cbi(II)$$

$$/\dot{S}^-Cbi(II)(pK_a = 5.2) + H_2O/H^+$$

1.3. Addition of second HS^- to Cbi(II):

$$(H\dot{S})Cbi(II)/\dot{S}^-Cbi(II) + HS^- \rightleftarrows \dot{S}SH^{2-}Cbi(II) + nH^+$$

The main product formed is a complex of Cbi(II) with $\dot{S}SH^{2-}$ [16]. Reduction of cobinamide yields a color change from red-orange (with a peak absorbance at ~510 nm) to a pale yellow observed (in Supplementary information; Fig. S1). Here, the distinct spectral shifts exhibited by the reaction of Cbi with H_2S was used to generate a simple paper-based diffuse reflectance sensor. Cobinamide [$OH(H_2O)Cbi$] was chosen as the indicator because it has a high affinity for HS^- and is currently under study as a H_2S-poisoning antidote [17]. Recently, Cbi [$CN(H_2O)Cbi$] on paper showed rapid detection of hydrogen cyanide (HCN) with characteristic spectral shifts at 583 nm [19]. Here, $OH(H_2O)Cbi$ on paper will be used to study the effects of reaction with H_2S to determine if a dual-ESLI could be developed, or if an interfering effect from H_2S would occur.

2. Experimental

2.1. Chemicals and materials

Aquohydroxocobinamide, [$OH(H_2O)Cbi$],(Co(III)) was synthesized from hydroxocobalamin as previously described [20]. A bench-top ultraviolet-visible (UV–vis) spectrometer (Thermo Scientific Evolution 300) was used to determine the concentration of cobinamide stock solutions using a molar extinction coefficient of $2.8 \times 10^4\ M^{-1}\ cm^{-1}$ [21]. Sodium sulfide (Na_2S; flakes, technical) and ascorbic acid were purchased from Fisher Scientific and dissolved in 1 mM NaOH (Fisher Scientific, certified) or deionized water, respectively. Stock H_2S gas was purchased at concentrations of 1001 (±2%) ppm, 10.0 (±5%) ppm, and at >99% purity from Matheson. All gases were balanced in nitrogen. Gelman Sciences A/E Borosilicate Glass fiber filter paper (without binder, 330 μm thick, and 1 μm pore size) was used as the support media. Deionized water was from an 18 MΩ-cm deionized in-line water system (Thermo Scientific Micropure). Cartridges designed for protection against H_2S were used for breakthrough experiments.

2.2. Preparation of paper substrates

Glass fiber paper was cut into uniform 6.0 ± 0.5 mm diameter circles. A volume of 15.00 ± 0.02 μL of 50.0 ± 0.2 μM Cbi was placed onto the center of each piece of paper leading to ~0.9 μg

OH(H_2O)Cbi per paper. The OH(H_2O)Cbi solution diffused uniformly across the paper circle and the wetted paper was allowed to dry fully for 1 h at room temperature (~21 °C). These conditions yielded a reflectance spectrum with acceptable signal-to-noise ratio at 500 nm (1.8×10^4). The spotted papers were stored at 4 °C.

2.3. Diffuse reflectance instrumentation

When light interacts with a paper's surface, the incidence light can be reflected, interreflected, refracted, absorbed, transmitted, or a combination of these events. Diffuse reflected light (or nondirectional reflectance) is reflected at many different angles due to light scattering. Diffuse reflectance occurs with rough surfaces, including soil [22], paint [23], body tissues [24], crystals [25] and paper [26,27]. A linear relationship of spectral intensity to sample concentration can be obtained from the Kubelka-Munk equation:

$$F(R) = \frac{(1-R)^2}{2R} = \frac{K}{S} \quad (1)$$

where R is reflectance, K is the absorption coefficient, and S is the scattering coefficient. The Kubelka-Munk equation is the most common approach to interpret diffuse reflectance and make the data comparable to that of transmittance [28].

An Ocean Optics USB4000 UV–vis-ES miniature spectrometer (200–850 nm) was used for diffuse reflectance measurements. Cbi-impregnated paper circles were inserted into a custom-made, light-tight holder constructed of black, Delrin® plastic described previously and shown in Fig. S2 [19]. Two holes in each side of the holder allowed H_2S to pass through the holder. The common end of a bifurcated fiber optic (Ocean Optics, core diameter 600 μm, fused silica) was connected to the bottom of the holder directly under the filter paper. The two distal branches of the fiber were connected to a tungsten halogen light source (Ocean Optics LLS, 215–2500 nm) and the USB spectrometer, respectively.

2.4. System optimization

Integration time for individual scans was set at 300 ms to yield a signal that was 85% of the spectrometer's saturation value (limited by the A/D converter to 65k counts), while the number of scans-to-average was chosen to optimize signal-to-noise. The spectrometer software measures the intensity of reflected light returning to the detector from the paper and converts the data to an apparent absorbance; the term "apparent absorbance" is used here because the configuration is not in a traditional transmittance configuration, rather a reflectance configuration to reduce the overall footprint of the sensor. Apparent absorbance was converted to reflectance (Eq. (2)) and then to the Kubelka-Munk Function (Eq. (1)) by:

$$R = 10^{-A} \quad (2)$$

where A is absorbance. Thus, the diffuse reflectance spectra—plotted as $F(R)$—will be used to study the spectral shifts upon H_2S exposure to Cbi.

2.5. H_2S flow experimental setup

All H_2S exposure experiments were performed at the NIOSH/NPPTL facility in Pittsburgh, PA; full explanation of testing can be found online [29]. Two Interscan® electrochemical instruments (Model RM-17-0 and RM-17-2) specific to H_2S were used with detection ranges of 0.00–19.99 ppm (resolution 0.01 ppm) and 0–1000 ppm (resolution 1 ppm), respectively. The 0.00–19.99 Interscan® was used for the initial H_2S exposure experiments and to monitor effluent breakthrough concentrations from NIOSH-approved canisters. This detector was calibrated with the 10.00 ppm H_2S gas. The 0–1000 ppm Interscan® was used to verify the H_2S challenge concentration throughout breakthrough experiments and was calibrated with the 1001 ppm H_2S. Gas flow was controlled from a PC using a LabVIEW virtual instrument program (National Instruments). Percent relative humidity (%RH), temperature, test time, challenge and breakthrough H_2S concentration were stored by the software. Each instrument was calibrated before the start of each experiment.

The system was initially flushed with clean air (oil-free compressed air) at the desired %RH (no H_2S) for 1 h before each experiment and was evaluated by the electrochemical detector to ensure an initial reading of 0.00 ppm H_2S. A blank paper circle was placed in the sensor holder and the reflectance signal was defined as 100% reflectance at each wavelength. A piece of OH(H_2O)Cbi-impregnated paper was then placed in the holder and the appropriate reflectance spectrum recorded. In some experiments, the reflectance spectrum of the OH(H_2O)Cbi-impregnated paper was designated as the "blank" when the goal was to monitor changes in the OH(H_2O)Cbi spectrum, termed "difference spectra". For the purpose of this proof-of-concept, 10.0 ppm H_2S was the concentration of interest to expose to the Cbi paper sensor. This is because it is the NIOSH REL. Additional studies will be undertaken for further H_2S concentrations. Relative humidity levels of 25, 50, and 85%RH at 25.0 °C ± 2.5 °C were tested, which are standard %RH in NIOSH/NPPTL certification protocol [30]. These humidity values were evaluated because respirators are used in a wide range of climates with various temperatures and humidity. Air was pulled to the sensor at 1.0 (±5%) liters per minute (LPM) to avoid back pressure build-up in the sensor holder. This flow rate does not simulate air flow through a canister, but was chosen for convenience to focus on studying the binding between H_2S and OH(H_2O)Cbi.

Three pairs of cartridges used for breakthrough studies were tested at 25 °C ± 2.5 °C at each of the three values of RH. The cartridges used were NIOSH-approved for protection against H_2S exposure, and were used per manufacturer-defined configurations. Each test was run at a continuous airflow of 64 LPM, with a challenge gas concentration of 1000 ppm H_2S. Each pair of cartridges was mounted into a test apparatus within an airtight testing chamber. A diverter valve allowed the challenge gas to flow into the testing chamber or to waste. The paper sensor (and associated spectrometer and light source) was placed on the effluent side of the cartridge. Air was pulled over the sensor at 1.0 LPM (±5%) by a Gilian Air Sampling Pump (GilAir-3) from the downstream flow of the cartridges. The test ran until breakthrough of 15.0 ppm H_2S was detected by the Interscan®. Data will be presented for 10.0 ppm H_2S, the C REL. Apparent absorbance spectra were obtained at 0, 10, 30, 45 min (for higher %RH), and at 10.0 ppm H_2S breakthrough (time varied for each pair of cartridges). One pair of pre-exhausted cartridges (at 25%RH) were stored in an airtight bag for 24 h and re-exposed to H_2S to determine if the Cbi paper sensor could rapidly detect imminent breakthrough.

3. Results and discussion

3.1. Paper substrate

Glass fiber filter paper was used as the sensor medium; in previous studies, this specific type of paper demonstrated larger reflectance signals, presumably because it is thicker than traditional cellulose filter paper and allowed more light to reach the detector in the presented reflectance configuration [19]. Additionally, glass fiber filter paper is less affected by water vapors. The concentration of Cbi concentration (50.0 ± 0.2 μM) was chosen to directly compare results with previously performed experiments of similar nature using HCN gas [19]. This Cbi concentration on paper was sufficient in detecting small changes in the Cbi reflectance

spectrum; higher concentrations of Cbi on paper decreased the sensitivity to slight changes in H_2S concentration upon exposure, where lower Cbi concentrations had undesirable signal-to-noise ratios.

3.2. UV–vis spectra of Cbi and Na_2S

Fig. 2 shows the absorbance spectra of a 50 μM OH(H_2O)Cbi solution on adding increasing amounts of Na_2S in 1 mM NaOH. The increase in absorbance from 400–450 nm, decrease from 470–550 nm, and isosbestic points near 470 and 550 nm are similar to those reported for H_2S in solution under anaerobic conditions [16]. The absorption spectrum of the 50 μM OH(H_2O)Cbi solution is similar to the diffuse reflectance spectra (plotted using the Kubelka-Munk function) of OH(H_2O)Cbi on glass fiber paper (Fig. S3).

3.3. Cbi detection of H_2S

The average apparent absorbance of OH(H_2O)Cbi on glass fiber paper (measured at 500 nm) was 0.15 ± 0.02 (F(R) value equal to 0.08 ± 0.02) with uncertainty in terms of 95% confidence interval. A 13% relative standard deviation (RSD) was reported for $n = 7$. The spectral changes that occurred on adding 100.0 μM Na_2S to a OH(H_2O)Cbi solution and exposing Cbi-impregnated paper to 10.0 ppm H_2S for 1 min at 25%RH under aerobic conditions (diffuse reflectance) were directly compared and are similar (Fig. 3). Fig. 4 shows the response of OH(H_2O)Cbi on paper (plotted as the Kubelka-Munk function) when exposed to 10.0 ppm H_2S for 1, 5, and 10 min at 25%RH, where the initial spectrum of OH(H_2O)Cbi on paper was considered the blank (considered difference spectra). The increased signal at 400–450 nm, decreased signal at 470–550 nm, and isosbestic points near 470 and 550 nm are apparent and similar to those previously reported [16]. F(R) versus time of 10.0 ppm H_2S exposure can be seen in Fig. S4.The average $F(R)$ values from 400–450 nm increases, while those from 470–550 nm decrease upon H_2S exposure.

The responses of Cbi exposed to 10.0 ppm H_2S (using OH(H_2O)Cbi) and 5.0 ppm HCN (using CN(H_2O)Cbi) for 10 min exposure at 25%RH were compared and shown in Fig. 5 (experiments performed separately) [19]. 5.0 ppm is the NIOSH REL for HCN. Cbi has a high affinity for CN^- (10^{14}) and has been used to detect cyanide gas [18]. Different spectral shifts of the Cbi complex were observed for exposure to these two gases. A dual-ESLI sensor could potentially be developed for detection of both HCN and H_2S with identification of HCN by the characteristic signal at 583 nm (i.e., formation of dicyanocobinamide), and H_2S by the increase between 400–450 nm, isosbestic point near 470 nm, and absence of an isosbestic point at 531 nm (observed upon formation of dicyanocobinamide). The average blank signal of Cbi on glass fiber paper measured at 531 nm in terms of the Kubelka–Munk function is $3\ (\pm 7) \times 10^{-7}$. Statistically, the limit of detection (LOD) in terms of the Kubelka-Munk function is 2.4×10^{-6} or 0.002 in terms of absorbance, using LOD = $3\sigma \pm x$.

3.4. Effect of %RH on H_2S detection

Increasing the %RH to 50% increased the signal from 400–450 nm and decreased F(R) signal from 470–550 nm. The spectral shifts for 10.0 ppm H_2S at 50%RH are similar to those at 25%RH, but at higher $F(R)$ values, suggesting binding of one or two HS^- groups to Cbi forming (HS)(H_2O) Cbi, or $(HS)_2$Cbi, respectively (Fig. S5). This observation may be attributed to water vapor adsorption by the paper, which may create a more solution-like medium for the reaction between H_2S and Cbi [31]. $F(R)$ versus time exposure are shown in in Fig. S6. The higher response could also be due to a smaller scattering cross-section for glass fiber paper as water fills the air-filled pores of the paper [31]. A small increase in signal from 550–700 nm was observed, which would cause a false positive error in detecting HCN using the characteristic 583 nm peak; data processing would be required upon sensor development. A comparison of Cbi detection for 10.0 ppm H_2S and 5.0 ppm HCN at 50%RH is shown in Fig. S7. The small increase from 550–700 nm observed for higher HS^- concentrations [16], and here in ascorbic acid under both aerobic and anaerobic conditions. The formation of Cbi(II) using another reducing agent, glucose, also shows a small increase in signal at ~600 nm, with further formation of Cbi(I) showing an increase from 600–800 nm [32].

The spectral shifts observed for 85%RH varied from those at 25 or 50%RH. For comparison, ascorbic acid reduction of OH(H_2O)Cbi under aerobic (i.e., occupationally-relevant situations, Fig. 6) and anaerobic (Fig. S8) conditions showed similar spectral shifts. Bubbling H_2S through a cobinamide solution decreases absorbance at 349 and 520 nm, increases absorbance at 314 and 468 nm and generates isosbestic points at 470 and 550 nm (anaerobic conditions) [16]. Comparing the spectral shifts of reducing reagents (in solution) and H_2S (gas phase) indicates the spectral shifts were due to reduction of Cbi, presumably to the 2+ oxidation state. Additionally, spectral shifts of Cbi reaction with both glucose and nitric oxide (NO) as reducing agents reported an absorbance peak at 469 nm indicating formation of Cbi(II), similarly observed here at 85%RH [32,33]. Other reducing agents reported to reduce vitamin B_{12} and cause similar spectral shifts include fructose [32], sodium borohydride [34], dithiothreitol [33], and sodium formate [34,35]. Gas phase reducing agents will generally not be present in occupationally-relevant environments, with the possible exception of carbon monoxide, which reacts extremely slowly with vitamin B_{12} (Co(II)) [36]. Therefore, carbon monoxide is not likely to cause an interference when using Cbi as the indicating reagent. Solution experiments were performed only for comparison of spectral shifts for Cbi + H_2S in the gas phase. Control experiments performed with OH(H_2O)Cbi on glass fiber paper at 85%RH and 0.0 ppm H_2S did not show changes to the Cbi spectrum. Thus, the spectral shifts at higher %RH suggest reduction of Cbi(III) to Cbi(II) possibly forming [(H)S]Cbi(II), signifying a more effective reaction between H_2S and Cbi. A comparison of Cbi detection for 10.0 ppm H_2S and 5.0 ppm HCN at 85%RH are shown in Fig. S9.

3.5. H_2S breakthrough of cartridges

Breakthrough experiments were conducted to determine if the Cbi-based paper sensor could accurately detect H_2S breakthrough from cartridges. The sensor was placed downstream of the effluent gas and simultaneously compared with the Interscan® electrochemical detector. The average ($n = 3$) F(R) responses at 10 and 30 min, and at 10.0 ppm breakthrough at 25%RH are shown in Fig. 7a. Fig. 7b shows an example of the OH(H_2O)Cbi response at 400–450, 470–550, and 800 nm (used as reference for the entirety of the breakthrough experiment), plotted as 5 point moving average. The F(R) trends were simultaneously compared to the response from the H_2S-specific electrochemical detector. This detector's response is plotted as the second derivative of the concentration vs. time to easily visualize the start of breakthrough (Fig. 7b). The complete breakthrough curve for the electrochemical detector can be seen in Fig. 8. The Cbi-based sensor efficiently detected low H_2S concentrations breaking through respirator carbon beds, with increased slopes upon imminent breakthrough. The F(R) spectra at various time intervals were similar to those observed for direct exposure of H_2S to the Cbi paper sensor (no carbon bed). Slight variations (e.g., shift in isosbestic points) may be attributed to possible formation of byproducts from the reaction with chemical impregnants. Without quantitative instrumentation (e.g., mass spectrometer), the final products could not be identified. A small

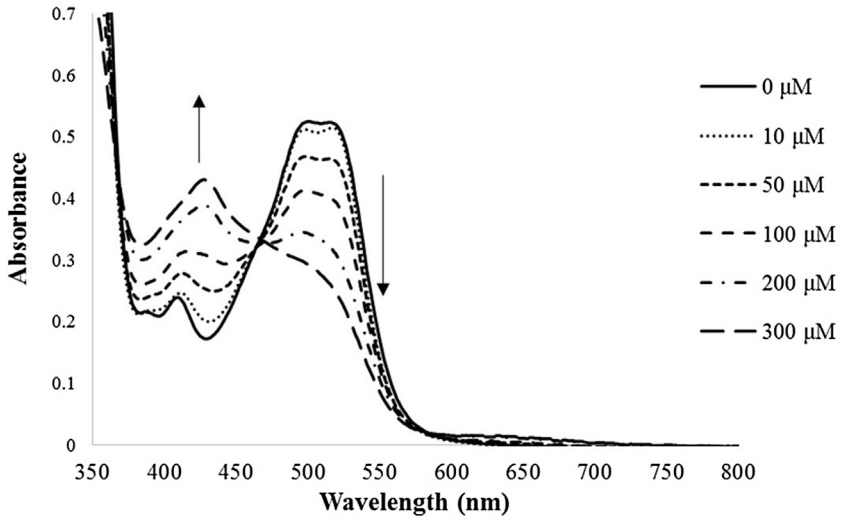

Fig. 2. Absorbance spectra of $OH(H_2O)Cbi$ (solid line) upon addition of 0.0–300.0 μM Na_2S.

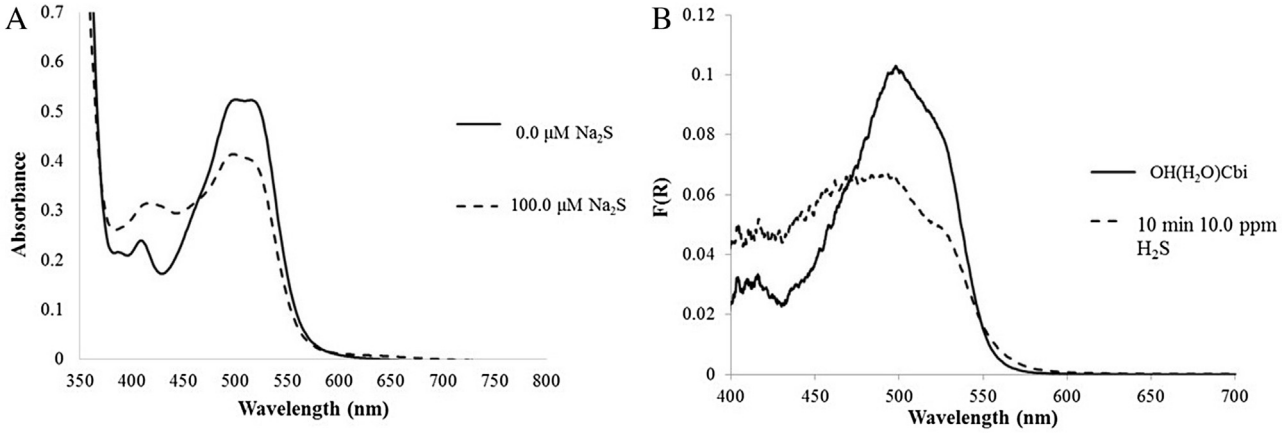

Fig. 3. Comparison of $OH(H_2O)Cbi$ solution spectra with Na_2S and diffuse reflectance spectra on glass fiber filter paper upon H_2S exposure. The Kubelka-Munk function is plotted for the diffuse reflectance spectra. (A) Aquohydroxocobinamide solution spectra for 50 μM $OH(H_2O)Cbi$ in solution before 100.0 μM Na_2S (solid line) and after Na_2S is added (dashed line). (B) Diffuse reflectance spectra for $OH(H_2O)Cbi$ on glass fiber paper before 10 min exposure to 10.0 ppm H_2S gas (solid line) and after H_2S exposure (dashed line).

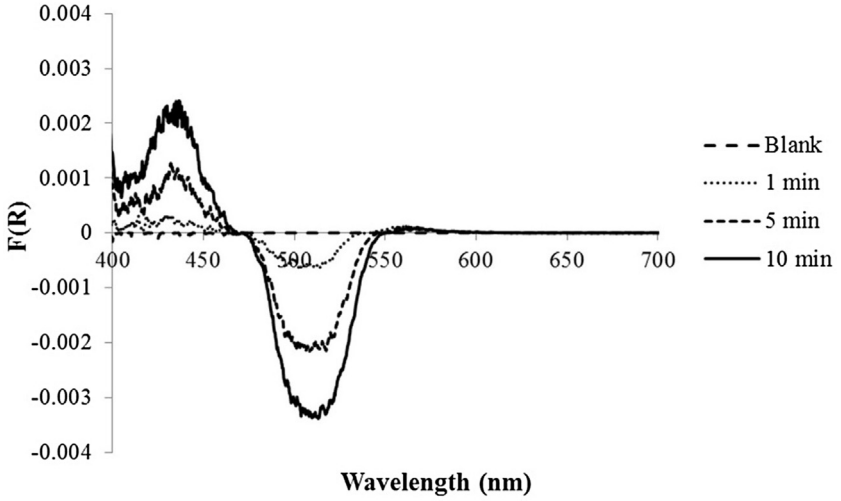

Fig. 4. Diffuse reflectance spectra where the reflectance spectrum of $OH(H_2O)Cbi$ on glass fiber filter paper was designated as the "blank" (long dashed line) and response to 10.0 ppm H_2S exposure on glass fiber filter paper as a function of time of exposure: 1 min of exposure (dotted line), 5 min of exposure (short dashed line), and 10 min exposure (solid line).

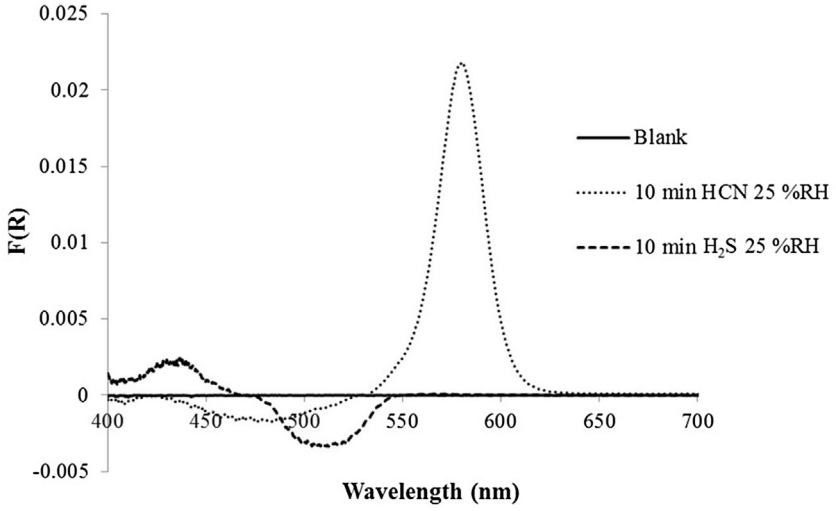

Fig. 5. Comparison of the diffuse reflectance spectrum of OH(H_2O)Cbi on glass fiber paper exposed to 10.0 ppm H_2S at 25%RH (dashed line) after 15 min and reflectance spectrum of CN(H_2O)Cbi on glass fiber paper exposed to 5.0 pm HCN at 25%RH (dotted line) after 15 min. OH(H_2O)Cbi on glass fiber paper was subtracted out and referred to as the blank (solid line).

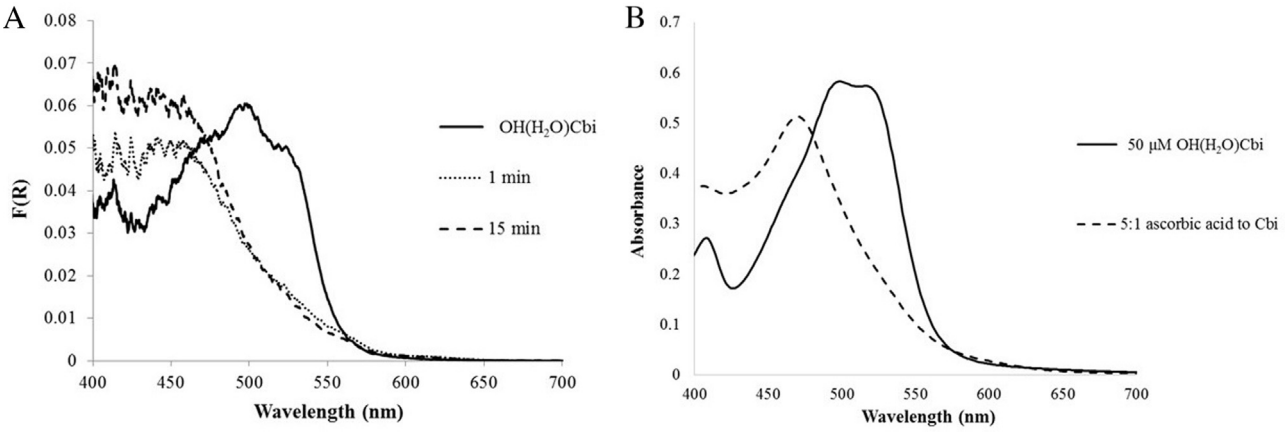

Fig. 6. (A) Diffuse reflectance spectrum of OH(H_2O)Cbi on glass fiber paper (solid line) and response to 10.0 ppm H_2S after 1 min (dotted line) and 15 min (dashed line). (B): UV–vis spectra of OH(H_2O)Cbi before (solid line) and after mixing with 5:1 ascorbic acid under aerobic conditions (dashed line).

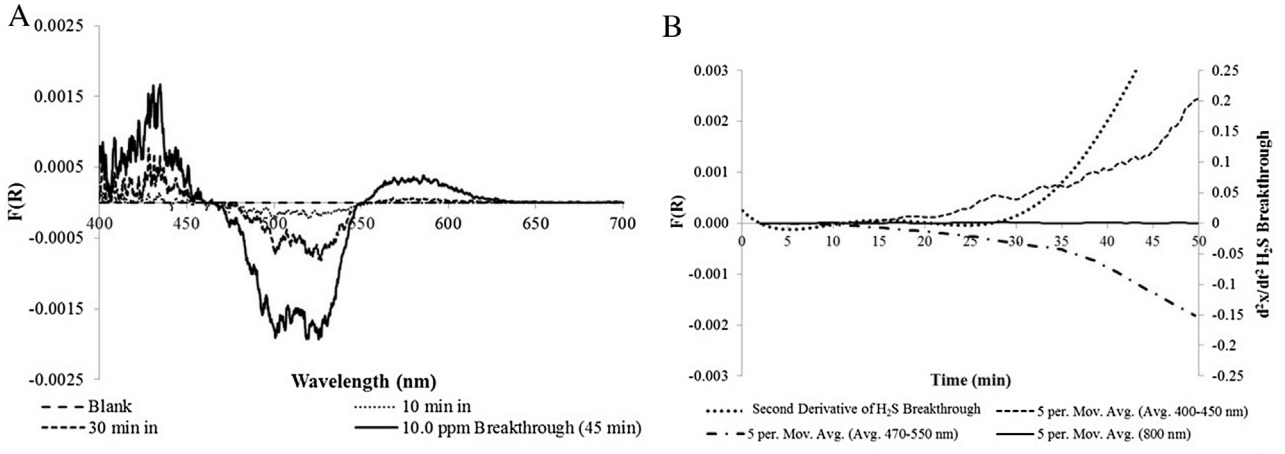

Fig. 7. (A) Average response of OH(H_2O)Cbi on glass fiber filter paper as a function of time of triplicate breakthrough experiments at 25%RH. Diffuse reflectance spectra were recorded at 10 and 30 min into experiment, and at 10.0 ppm H_2S breakthrough. (B). Direct comparison of breakthrough curves of the electrochemical detector (dotted line, plotted as the second derivative), and Cbi paper sensor at 400–450 nm response (short dashed line), 470–550 nm response (dot-dashed line) and 800 nm response (solid line, as the reference) plotted as 5-point moving averages. $T = 0$ represents time experiment started.

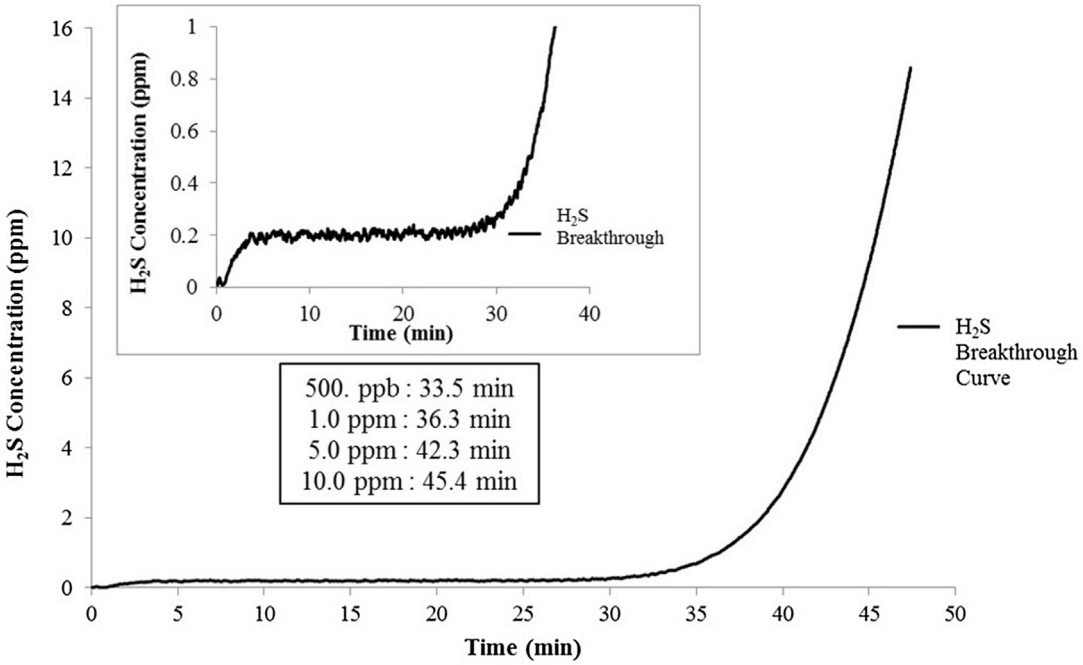

Fig. 8. Electrochemical detector breakthrough curve from the respirator cartridges used in Fig. 7b. Inset figure: Expansion of breakthrough curve at low concentrations of H_2S observed through entirety of experiment. Inset text box: H_2S concentration (ppm) at specific time points within experiment.

increase in baseline (correlating to ~200 ppb H_2S) was observed on the electrochemical detector readout throughout the majority of the tests (Fig. S11). This could be from a small amount of H_2S permeating through the carbon bed; this is common in cartridge testing varying significantly between brands and lots. The permeation could be attributed to vapor moving through the channels within the bed, or formation of chemical byproducts. The cumulative response—which would occur during a user's breathing—observed in the Cbi $F(R)$ breakthrough curves was most likely attributed to the small amount of H_2S breakthrough, though a quantitative change in slope was found upon imminent breakthrough. Cbi also successfully detected breakthrough of HCN from respirator canisters where the $F(R)$ response at 583 nm is plotted against the electrochemical detector response (Fig. S11a). The diffuse reflectance response at various times throughout the experiment can be seen in Fig. S11b where the spectral shifts are distinctively different than that of H_2S breakthrough—there is no increase from 400–450 nm and no change at 531 nm. HCN breakthrough experiments will be published elsewhere.

Longer breakthrough times were observed as a function of increased %RH. This is due to the solubility between H_2S and water vapor that is adsorbed to the active sites of the activated carbon. Both sensors detected low concentrations of H_2S, suggesting the paper sensor could detect imminent breakthrough in the desired amount of time. Larger $F(R)$ values and closer correlation between the Cbi-based paper sensor and electrochemical sensor were observed for cartridges exposed to 10.0 ppm H_2S at 85%RH breakthrough (Fig. 9 and Fig. S12). Although only one concentration of H_2S was studied for direct exposure to Cbi on paper (i.e., 10.0 ppm H_2S), the Cbi paper sensor clearly shows detection at lower concentrations upon imminent breakthrough of a carbon bed (less than 1.0 ppm according to the H_2S-specific electrochemical detector). Unlike traditional chemical sensors, a respirator ESLI must show response at a pre-determined concentration/location within the carbon bed. For an H_2S-specific ESLI, this would be at 10.0 ppm H_2S.

A cartridge that had prior breakthrough was also tested to determine if the paper sensor could rapidly detect H_2S on re-breakthrough, a hazardous situation when intermittent cartridge use occurs. Breakthrough did not occur immediately for this cartridge, suggesting H_2S had redistributed on the carbon and allowed a small increase in service-life. However, breakthrough occurred within 8.5 min compared to 45 min for a fresh cartridge pair (at 25%RH). The average response of Cbi on paper from 400–450 nm and 470–550 nm corresponded well with the electrochemical detector (Fig. 10).

The data suggest that Cbi on paper can rapidly detect imminent H_2S breakthrough which would indicate to the user that the cartridge must be immediately replaced, as per ESLI standards and user instructions [7,37]. The sensor could eventually be incorporated into the carbon bed of a cartridge to detect, at minimum, 10% service-life remaining. The requirements for ESLIs in respirators are unlike those for conventional chemical sensors. Although the reaction of Cbi with H_2S is reversible, the event and indication of a gas/vapor reaching 90% within the cartridge needs to occur only once, thus an ESLI does not have to show reversibility [2].

4. Conclusions

An inexpensive paper-based optochemical sensor was developed for detecting low concentrations (10.0 ppm) of H_2S gas. Due to the low cost, small size, and ability to detect the NIOSH-recommended C REL concentration for H_2S gas, the sensor has potential to be used as an ESLI in respirators. Distinct spectral shifts were observed for the reaction of one or two HS^- groups binding to aquohydroxocobinamide, and the possible reduction of the Cbi(III) complex under conditions of higher humidity.

The Cbi sensor detected H_2S breakthrough from cartridges and breakthrough curves correlated well with a commercially available, H_2S-specific electrochemical detector. Therefore, incorporating the sensor into a cartridge and combining it with a warning signal (e.g., LED) could indicate to the user that the cartridge service-life has almost ended and that the cartridge must be replaced immediately.

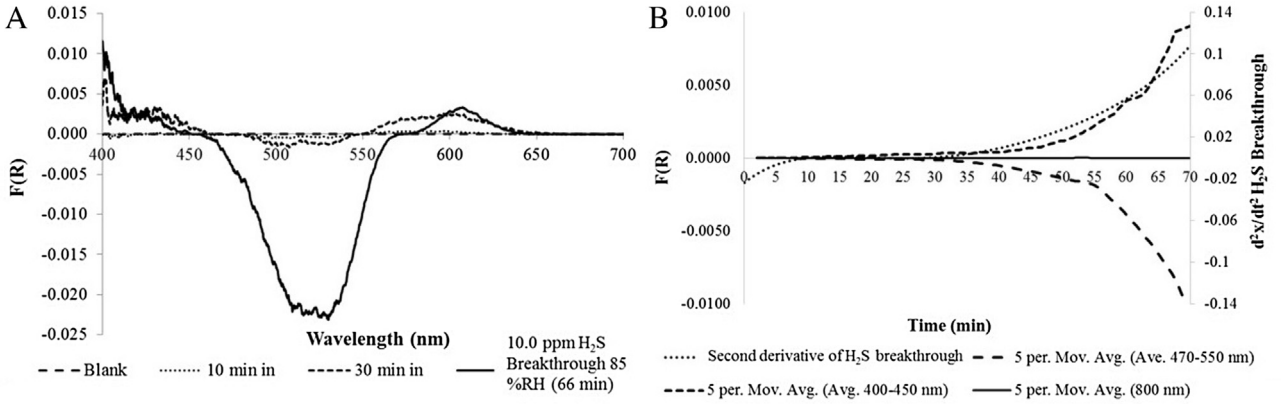

Fig. 9. (A) Average response of OH(H_2O)Cbi on glass fiber filter paper as a function of time into triplicate breakthrough experiments at 85%RH. (B) Direct comparison of breakthrough curves of the electrochemical detector (dotted line, plotted as the second derivative), and Cbi paper sensor at 400–450 nm response (short dashed line), 470–550 nm response (long dashed line), and 800 nm response (solid line, as the reference) plotted as 5-point moving averages. $T = 0$ represents time experiment started.

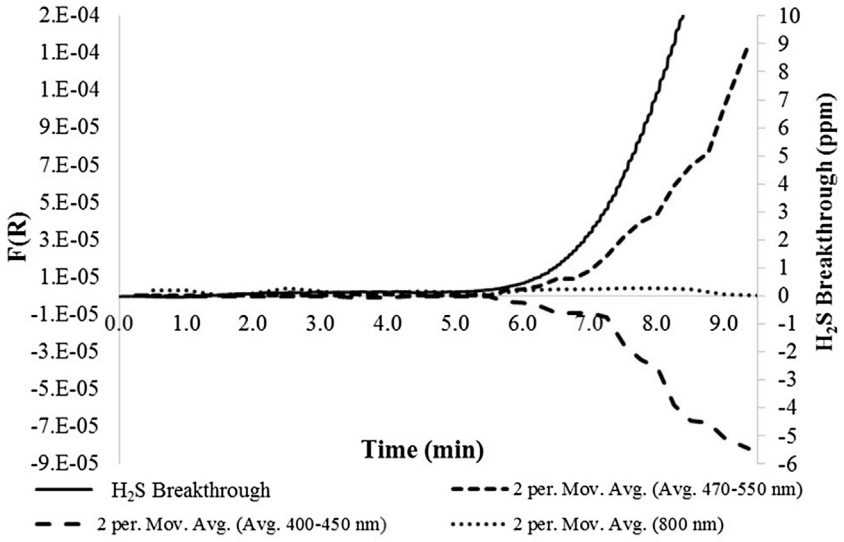

Fig. 10. Breakthrough curve of the pre-exhausted pair of cartridges at 25%RH. Direct comparison of breakthrough of the electrochemical detector (solid line) and Cbi paper sensor at 400–450 nm response (short dashed line), 470–550 nm response (long dashed line), and 800 nm response (dotted line, as the reference) plotted as 2-point moving averages.

The availability of small photodetectors, inexpensive optical fibers, and battery-powered LED light sources suggest that the simple diffuse reflectance configuration could be miniaturized to satisfy the size, cost, and power requirements of ESLIs. The paper medium and diffuse reflectance configuration is versatile and could be used for other gas colorimetric indicators. Soon to be reported elsewhere, the Cbi paper sensor also accurately detects breakthrough of HCN (and cyanogen) through CBRN respirator canisters.

Author contributions

The manuscript was written through contributions of all authors. All authors have given approval to the final version of the manuscript.

Disclaimer

The findings and conclusions in this report are those of the authors and do not necessarily represent the views of the National Institute for Occupational Safety and Health. Mention of product name does not constitute endorsement by the National Institute for Occupational Safety and Health or the Centers for Disease Control and Prevention.

Acknowledgment

The authors acknowledge financial support from CDC/NIOSH/NPPTL, and from the Office of the Director, NIH, and NINDS Grant #U01 NS058030 for the funding of this project. First author would like to acknowledge Jay Snyder, Dr. Nicole Fry, Dr. Michael Sailor, and Dr. Harry Finklea for insightful discussions that were essential to this manuscript.

Appendix A. Supplementary data

Supplementary data associated with this article can be found, in the online version, at http://dx.doi.org/10.1016/j.snb.2016.02.129.

References

[1] NIOSH, Hydrogen Sulfide, NIOSH Pocket Guide to Chemical Hazards, 2015, Retrieved from http://www.cdc.gov/niosh/npg/npgd0337.html (accessed 09.21.15).

[2] G.J. Maclay, M.W. Findlay, J.R. Stetter, A prototype active end-of-service-life indicator for respiratory cartridges, Appl. Occup. Environ. Hygiene 6 (1991) 677–682.
[3] OSHA, Regulations (Standards-29CFR). Retrieved from https://www.osha.gov/pls/oshaweb/owadisp.show_document?p_id=12716&p_table=STANDARDS (accessed 08.10.15).
[4] CDC, End-of-Service-Life 2012 Retrieved from http://www.cdc.gov/niosh/npptl/topics/respirators/disp_part/RespSource3end.html (accessed 05.08.15).
[5] S. Rose-Pehrsson, M.L. Williams, Integration of Sensor Technologies in Respirator Vapor Cartridges as End-of-Service Life Indicators: Literature and Manufacturers Review and Research Roadmap (2005).
[6] N.J. Bollinger, R.H. Schutz, NIOSH Guide to Industrial Respiratory Protection, Cincinnati OH (1987).
[7] NIOSH, Determination of End of Service Life Indicator (ESLI) Test, Air-Purifying Respirators Standard Testing Procedure (STP), Pittsburgh, PA (2005).
[8] N. Honeywell, N Series Catridges and Filters Retrieved from http://www.honeywellsafety.com/Products/Respiratory_Protection/N_Series_Cartridges_Filters.aspx?site=/&LangType=1033 (accessed 02.23.15).
[9] North, Cartridge and Filter Reference Chart Catridge and filter Reference Chart. Retrieved from http://www.unitedfireandsafety.com/Userfiles/Docs/Cartridge_Filter_Chart.pdf (accessed 02.23.15).
[10] B. Doujaiji, J.A. Al-Tawfig, Hydrogen sulfide exposure in an adult male, Ann. Saudi Med. 30 (2010) 76–80.
[11] Occupational Safety and Health Administration, Hydrogen Sulfide Retrived from https://www.osha.gov/SLTC/hydrogensulfide/standards.html (accessed 05.05.15).
[12] Occupational Safety and Health Administration OSHA Fact Sheet: Hydrogen Sulfide (H_2S), Retrived from https://www.osha.gov/OshDoc/data_Hurricane_Facts/hydrogen_sulfide_fact.pdf (accessed 11/10/15).
[13] X. Hu, B. Mutus, Electrochemical detection of sulfide, Rev. Anal. Chem. 32 (2013) 247–256.
[14] MSA Gas Monitors, MSA Altair Pro Single-Gas Detector- Hydrogen Sulfide, Retrived from http://www.msagasmonitors.com/10074136.html (accessed 05.15.15).
[15] Grainger, Hydrogen Sulfide (H_2S) Gas Detectors Retrieved from http://www.grainger.com/category/ecatalog/N-1z0dwuc (accessed 09.21.15).
[16] D.S. Salnikov, S.V. Makarov, R. van Eldik, P.N. Kucherenko, G.R. Boss, Kinetics and mechanism of the reaction of hydrogen sulfide with diaquacobinamide in aqueous solution, Eur. J. Inorg. Chem. (2014) 4123–4133.
[17] M. Brenner, S. Benavides, S.B. Mahon, J. Lee, J. Yoon, D. Mukai, et al., The vitamin B12 analog cobinamide is an effective hydrogen sulfide antidote in a lethal rabbit model, Clin. Toxicol. 52 (2014) 490–497.
[18] J. Ma, P. Dasgupta, F.H. Zelder, G.R. Boss, Cobinamide chemistries for photometric cyanide determination. A merging zone liquid core wavequide cyanide analyzer using cyanoaquacobinamide, Anal. Chim. Acta 736 (2012) 78–84.
[19] L.A. Greenawald, J.L. Snyder, N.L. Fry, M.J. Sailor, G.R. Boss, H.O. Finklea, et al., Development of a cobinamide-based end-of-service-life indicator for detection of hydrogen cyanide gas, Sens. Actuators B: Chem. 221 (2015) 379–385.
[20] K.E. Broderick, V. Gingh, S. Zhuang, A. Kambo, J.C. Chen, V.S. Sharma, et al., Nitric oxide scavenging by the cobalamin precursor cobinamide, J. Biol. Chem. 280 (2005) 8678–8686.
[21] W.C. Blackledge, C.W. Blackledge, A. Griesel, S.B. Mahon, M. Brenner, R.B. Pilz, et al., New facile method to measure cyanide in blood, J. Anal. Chem. 82 (2010) 4216–4221.
[22] A.C. Samuels, C. Zhu, B.R. Williams, A. Ben-David, R.W. Miles, M. Hulet, Improving the linearity of infrared diffuse reflection spectroscopy data for quantitative analysis: an application in quantifying organophosphorous contamination in soil, J. Anal. Chem. 78 (2006) 408–415.
[23] L. Monico, K. Janssens, C. Miliani, G. Van der Snickt, B.G. Brunetti, M.C. Guidi, et al., Degradation process of lead chromate in paintings by vincent van gogh studied by means of spectromicroscopic methods. artificial aging of model samples of co-precipitates of lead chromate and lead sulfate, J. Anal. Chem. 85 (2013) 860–867.
[24] B. Yu, A. Sha, V.K. Nagarajan, G.G. Ferris, Diffuse reflectance spectroscopy of epithelial tissue with a smart fiber-optic probe, Biomed. Optics Express 5 (2014) 675–689.
[25] S.J. Lee, S.W. Han, H.J. Choi, K. Kim, Phase behavior of organic-inorganic crystal: temperature-dependent diffuse reflectance infrared spectroscopy of silver sterate, Eur. Phys. J. D 16 (2001) 293–296.
[26] V.H.M. Luiz, L. Pezza, H.R. Pezza, Determination of nitrite in meat products and water using dapsone with combined spot test/diffuse reflectance on filter paper, Food Chem. 134 (2012) 2546–2551.
[27] S.A. Momin, R. Narayanaswamy, Optosensing of chlorine gas using a dry reagent srip and diffuse reflectance spectrophotometry, Anal. Chim. Acta 244 (1991) 71–79.
[28] M.L. Myrick, M.N. Simcock, M. Baranowski, H. Brooke, S.L. Morgan, J.N. McCutcheon, The Kubelka-Munk diffuse reflectance formula revisited, Appl. Spectrosc. Rev. 46 (2014) 140–165.
[29] NIOSH, Determination of Hydrogen Sulfide Service-Life Test, Air-Purifying Respirators with Cartridges Standard Test Procedure (STP), Pittsburgh, PA (2008).
[30] NIOSH, Standard Respirator Testing Procedures, Retrived from http://www.cdc.gov/niosh/npptl/stps/apresp.html (accessed 06.10.15).
[31] A.K. Ellerbee, S.T. Phillips, A.C. Siegel, K.A. Mirica, A.W. Martinez, N. Striehl, et al., Quantifying colorimetric assays in paper-based microfluidic devices by measuring the transmission of light through paper, Anal. Chem. 81 (2009) 8447–8452.
[32] I.A. Dereven'kov, D.S. Salnikov, N.I. Shpagilev, S.V. Makarov, E.N. Tarakanova, Reactions of cobinamide with glucose and fructose, Macroheterocycles 5 (2012) 260–265.
[33] V.S. Sharma, R.B. Pilz, G.R. Boss, D. Magde, Reactions of nitric oxide with vitamin B_{12} and its precursor, cobinamide, Biochemistry 42 (2003) 8900–8908.
[34] M. Wolak, A. Zahl, T. Schneppensieper, G. Stochel, R. Van Eldik, Kinetics and mechanism of the reversible binding of nitric oxide to reduced cobalamin B_{12r} Cob(II) alamin), J. Am. Chem. Soc. 123 (2001) 9780–9791.
[35] D.E. Linn Jr., E.S. Gould, Electron transfer. 92. Reductions of vitamin $B12_a$ (Hydroxocobalamin) with formate and related formyl species, Inorg. Chem. 27 (1987) 1625–1628.
[36] L. Lee, G.N. Schrauzer, The Reaction of vitamin B_{12a} and of cobaloximes with carbon monoxide. Evidence for self-reduction of vitamin B_{12a} in neutral solution, J. Am. Chem. Soc. 90 (1968) 5274–5276.
[37] 3 M, Cartridge 6000 Series, 2016, Retrieved from http://multimedia.3m.com/mws/media/529757O/3m-6000-series-respirators-user-instructions.pdf (accessed 06.10.15).

Biographies

Lee A. Greenawald is a Ph.D. candidate in the C. Eugene Bennett Department of Chemistry at West Virginia University and a physical scientist student trainee at the National Institute for Occupational Safety and Health in Morgantown, WV. She received her B.S. degree in Forensic Chemistry from Ohio University in 2011. Her research interests include the development of inexpensive and portable sensors that have potential to be used with a respirator to protect users against breathing toxic gases. She has presented at various analytical and forensic-related conferences.

Gerry R. Boss is a Professor of Medicine at the University of California, San Diego. A major area of his research interest is in developing countermeasures to toxic chemicals. He found that cobinamide is not only an effective cyanide countermeasure, but also that it could be used to quantitatively measure low amounts of cyanide.

Aaron J. Reeder received a M.S. in Chemistry from Carnegie Mellon University. He has been with the National Institute for Occupational Safety and Health for the past five years and is the lead technician in the air purifying respirator certification laboratory

Suzanne Bell is an associate professor in the C. Eugene Bennett Department of Chemistry and in the Forensic and Investigative Sciences Department at West Virginia University. Her research interests are in applied and forensic analytical chemistry, chemometrics, and forensic toxicology.